Pharm Res (2014) 31:2516–2528
DOI 10.1007/s11095-014-1347-x

RESEARCH PAPER

Co-delivery of Sildenafil (Viagra®) and Crizotinib for Synergistic and Improved Anti-tumoral Therapy

João G. Marques • Vítor M. Gaspar • David Markl • Elisabete C. Costa • Eugénia Gallardo • Ilídio J. Correia

Received: 21 November 2013 / Accepted: 24 February 2014 / Published online: 13 March 2014

ABSTRACT

Purpose Cancer multi-drug resistance is a major issue associated with current anti-tumoral therapeutics. In this work, Crizotinib an anti-tumoral drug approved for the treatment of non-small lung cancer in humans, and Sildenafil (Viagra®), were loaded into micellar carriers to evaluate the establishment of a possible synergistic anti-tumoral effect in breast cancer cells.

Methods Micellar carriers comprised by PEG-PLA block co-polymers were formulated by the solvent displacement method in which the simultaneous encapsulation of Crizotinib and Sildenafil was promoted. Encapsulation efficiency was analyzed by a new UPLC method validated for this combination of compounds. Micelle physicochemical characterization and cellular uptake were characterized by light scattering and confocal microscopy. The bio- and hemocompatibility of the carriers was also evaluated. MCF-7 breast cancer cells were used to investigate the synergistic anti-tumoral effect.

Results Our results demonstrate that this particular combination induces massive apoptosis of breast cancer cells. The co-delivery of Crizotinib and Sildenafil was only possible due to the high encapsulation efficiency of the micellar systems (>70%). The micelles with size ranging between 93 and 127 nm were internalized by breast cancer cells and subsequently released their payload in the intracellular compartment. The results obtained demonstrated that the delivery of both drugs by micellar carriers led to a 2.7 fold increase in the anti-tumoral effect, when using only half of the concentration that is required when free drugs are administered.

Conclusions Altogether, co-delivery promoted a synergistic effect and demonstrated for the first time the potential of PEG-PLA-Crizotinib-Sildenafil combination for application in cancer therapy.

KEY WORDS anti-tumoral effect · block co-polymers · breast cancer · co-delivery · synergistic effect

INTRODUCTION

Breast cancer is currently one of the most diagnosed solid tumors in women (1). In 2010, nearly 1.5 million of women were affected worldwide by this disease (2,3). The currently available chemotherapies are still largely restricted due to their deleterious side effects and poor efficacy for late stages of disease (4). Such limitations are associated with the lack of specificity towards cancer cells, leading to drug partitioning in other tissues and organs, particularly in the liver, lungs, kidney and heart (5). This bottleneck significantly reduces the bioavailability of chemotherapeutics at the target tumor site and is also responsible for extending the period during which anti-tumoral drugs are administered to patients (6). Moreover, the rapid systemic clearance of drugs and the difficulty of penetrating into deep tumor regions further contributes for the ineffectiveness of the existing treatments (7). Delivery of current available chemotherapy agents through nanocarriers has demonstrated to increase their therapeutic effectiveness and prolong patient survival rates (8). In fact, the loading of chemotherapeutics in drug delivery systems, utterly modulates their pharmacokinetic/pharmacodynamic profiles, especially their serum half-life and bioavailability at the target site (8). Several different types of nanoparticles have been produced for this purpose with organic, inorganic or combinations of these materials (9,10). However, the toxicity, limited drug loading and retention are some of the drawbacks associated with the majority of these systems (9,10). Conversely, amphiphilic polymeric nanoparticles present excellent biocompatibility, possibility of chemical modification, increased drug

Electronic supplementary material The online version of this article (doi:10.1007/s11095-014-1347-x) contains supplementary material, which is available to authorized users.

J. G. Marques • V. M. Gaspar • D. Markl • E. C. Costa • E. Gallardo • I. J. Correia (✉)
CICS-UBI - Health Sciences Research Centre
Universidade da Beira Interior, Avenida Infante D. Henrique
6200-506 Covilhã, Portugal
e-mail: icorreia@ubi.pt

loading capacity and facile manufacturing, through self-assembly (11). Micelles produced with amphiphilic co-polymers are more stable in biological environments and more biocompatible in comparison to those formulated by surfactants, such as cetyltrimethylammonium bromide (CTAB) and sodium dodecyl sulphate (SDS) (12,13). In this unique core-shell architecture the drug is protected from biological degradation and its cytotoxic side effects are significantly reduced (14). Poly (ethylene glycol)-poly (lactic acid) (PEG-PLA), a Food and Drug Administration (FDA) approved delivery system, is one of the most used amphiphilic polymers due to its stealth capacity, granted by the PEG moiety, and high drug loading capacity, conferred by the hydrophobic interactions that occur between hydrophobic drugs and PLA chains (15). Chemotherapy agents such as, Doxorubicin, Daunorubicin and Mitoxantrone are commonly used for the treatment of breast cancer, but their continuous administration is responsible for the development of multi drug resistant cancer cells, restraining the effectiveness of these treatments (16,17). Such phenomenon is owed to the overexpression of efflux pumps, membranar proteins that shuttle chemotherapeutics to the extracellular medium (17). In this context, the strategy of co-administration of two or more drugs for cancer therapy has tremendous advantages since synergistic therapeutic effects can be obtained for cancer therapy, as previously described in literature (18,19). However, the limited drug bioavailability and pharmacokinetics when administered intravenously in its free form, still hampers this approach. The use of nanotechnology in co-delivery has demonstrated successful results, specially using micellar carriers (20). Lee *et al.* 2009, reported a synergistic effect between Paclitaxel and Herceptin when delivered to breast cancer cells through cationic micellar nanoparticles (21). Zhang *et al.* 2007, have achieved similar synergistic effect when co-delivering Doxorubicin and Docetaxel to prostate epithelial cells by using polymeric micellar vehicles (20).

However, some of these drugs still have side effects a fact that compromises their usage and forces the finding of new strategies and synergies. In this context, Crizotinib (PF-2341066), an anti-tumoral drug that has been recently approved by the FDA for non-small lung cancer arises as an interesting bioactive molecule to be used also in breast cancer therapy (22). Crizotinib, acts as a potent inhibitor of c-MET a gene that encodes for the hepatocyte growth factor receptor (HGFR), and also of anaplastic lymphoma kinase (ALK) phosphorylation, and has also the ability to induce apoptosis via Caspase-3, as well an anti-angiogenic potential (23). Furthermore, it is also described that this drug specifically inhibits the MDR1 efflux transporter, coded by ABCB1 gene, both *in vitro* and *in vivo* (24). Therefore, it is highly valuable to explore its simultaneous co-delivery with other drugs that have a broad spectrum of inhibition of ATP-binding cassette (ABC) transporters, in order to promote an improved effect (25). Sildenafil, a potent phosphodiesterase inhibitor, also possess an antagonist effect on ABC efflux pumps, since it inhibits the action of MDR1, breast cancer resisting protein (BCRP) and multidrug resistance-associated protein 1 (MRP1), which are present in breast cancer cells (26). In this work, a synergistic anti-tumoral effect was achieved when Crizotinib and Sildenafil were simultaneously delivered through PEG-PLA micellar vehicles to breast cancer cells.

MATERIALS AND METHODS

Materials

Metoxy Poly (ethylene glycol) (mPEG) 2000 was obtained from Nanocs (New York, USA). Dulbecco's Modified Eagle's Medium (DMEM), Resazurin and Rhodamine B Isothiocyanate (RITC) were acquired from VWR Internacional (Carnaxide, Portugal). MCF-7 (ATCC® HTB-22) mammary gland adenocarcinoma cell line was obtained from ATCC (Middlesex, United Kingdom) and primary normal human dermal fibroblasts (hFIB) from Promocell (Heidelberg, Germany). Stannous Octoate ($Sn(Oct)_2$) was purchased from (Cymit Química, Barcelona, Spain). PF-02341066 (Crizotinib) and PF-4540124 (Sildenafil) were purchased from Tocris Bioscience (Nortpoint, United Kingdom). CellEvent™ Caspase-3/7® and Hoechst 33342® were obtained from Invitrogen (Carlsbad, USA). L-Lactide monomer and Pyrene were acquired from TCI (Tokyo Chemical Industry, Co., LTD., Japan). 3-(4,5-dimethylthiazol-2-yl)-5-(3-carboxymethoxyphenyl)-2-(4-sulfophenyl)-2H-tetrazolium) (MTS) was obtained from Promega (Madison, WI, USA). Phalloidin CruzFluor® 647 was obtained from Santa Cruz Biotechnology (Santa Cruz Biotechnology, Santa Cruz, Canada).

Methods

Synthesis of mPEG-PLA

The polymerization process of PEG-PLA co-polymers was performed as described previously in the literature (27). Initially, a 1:305 molar ratio of mPEG:L-LA were weighted into a reaction flask. Afterwards, dry toluene was injected in the reaction flask followed by the addition of $Sn(Oct)_2$ (0.1%). Ring Open Polymerization (ROP) was carried out at 120°C for 8 h. The resulting product was dissolved and recovered by precipitation, in methanol (MetOH). The block co-polymer was afterwards dialyzed during 5 days and freeze-dried (Scanvac CoolSafe™, ScanLaf A/S, Denmark).

Nuclear Magnetic Resonance

^1H Nuclear Magnetic Resonance (NMR) spectra was acquired in a Brüker Advance III 400 MHz spectrometer

(Brüker Scientific Inc, USA) using Deuterated Chloroform ($CDCl_3$) as solvent. The recorded spectra were processed with the TOPSPIN 3.1 software (Brüker Scientific Inc). All the assignments in ^1H NMR spectra were performed in accordance to the chemical shifts previously reported in the literature (28). The number average molecular weight (Mn) of the PLA chain and the degree of polymerization of PLA were determined as previously described by Li and co-workers (28). A total of five replicates were performed.

Micelle Self-Assembly - Film Hydration Method

PEG-PLA micelles were formulated via the film-hydration method (also known as solvent displacement method), as described in the literature (29). For micelle self-assembly, 10 mg of PEG-PLA block co-polymers dissolved in 1 mL of a 1:1 (v/v) mixture of Dicloromethane (DCM)/MetOH and transferred to a round-bottom flask. 2.22×10^{-8} mol of Crizotinib/mg of polymer (100 μg of Crizotinib dissolved in MetOH) were added to the mixture, which was evaporated (Rotavap® R-215, Büchi, Switzerland), subsequently hydrated with 1 mL of ultrapure water, sonicated for 30 min (Branson Ultrasonic Corp., CT, USA) and further recovered by centrifugation (30,000 × *g*, 40 min). The self-assembly of dual drug loaded micelles was also prepared with this methodology by adding also 100 μg of Sildenafil (MetOH) in the first step, simultaneously with Crizotinib. Following the terminology used above to name micelles, drug loaded micelles are termed as PL C (Crizotinib loaded PEG-PLA micelles) and PL CS (Crizotinib and Sildenafil loaded PEG-PLA micelles).

Determination of the Critical Micellar Concentration

The critical micellar concentration (CMC) of the different PEG-PLA co-polymers was determined by using pyrene (0.6 μM) as previously described elsewhere (30). To calculate the CMC different polymer concentrations ranging from 0.001 to 2,000 μg/mL were used. Fluorescence was monitored on a Spectramax Gemini XS spectrofluorometer (Molecular Devices LLC, USA) as reported by Layek and co-workers (30).

Haemolysis Assay

Red Blood Cells (RBC) extracted from Wistar rats were incubated with a range of concentrations (50 and 500 μg/mL) of PEG-PLA micelles for 1 h, at 37°C. Phosphate Buffer Saline (PBS) and Triton-X100 incubated RBC's were used as negative and positive controls, respectively. The determination of free haemoglobin was performed by ultraviolet-visible (UV-vis) analysis at $\lambda = 540$ nm (Shimadzu Inc., Japan). Additionally, the integrity of the RBC's was also characterized by Scanning Electron Microscopy (SEM). For this analysis RBC's were prepared as previously described by Akgül *et al.* 2010 (31). The dehydrated RBCs were dispersed in a cover glass for posterior SEM analysis as described below.

Encapsulation Efficiency and Release Profile Samples Analysis

Encapsulation efficiency was quantified through chromatographic analysis by using an Agilent 1200 Ultra Performance Liquid Chromatography (UPLC) system, equipped with an Agilent 1290 Infinity Detector (G4212A DAD). All the chromatographic runs were performed in an Agilent Zorbax Eclipse C_{18} column (5 μm, 4.6×150 mm) (Agilent Technologies, CA, USA), at 30°C. For UPLC analysis the remaining supernatants, after particle recovery, were injected in the column. Traces of drugs that could remain in the balloon used for micelle assembly were also analyzed. The encapsulation efficiency of both Crizotinib and Sildenafil was then calculated as follows:

$$\text{Encapsulation Efficiency } (\%) = \frac{\left([\text{Drug}]_{\text{initial}} - \left([\text{Drug}]_{\text{supernatant}} + [\text{Drug}]_{\text{flask}}\right)\right)}{[\text{Drug}]_{\text{initial}}} \times 100$$

The method for dual drug quantification was optimized from a method previously described for Sildenafil (32). The mobile phase used for the chromatographic runs was composed of Na_2HPO_4 (0.015 M pH 7.4) and 0.01% Triethylamine (TEA) (v/v). Sample analysis was performed using the isocratic mode at a constant flow rate of 1 mL/min, at 30°C.

Morphological Characterization of PEG-PLA Micelles

Self-assembled micelles morphological properties were visualized by SEM. For this purpose, dried micelle preparations were mounted on aluminium stubs and sputter coated with gold with an Emitech K550 sputter coater (Emitech Ltd, UK). The nano sized carriers where then observed on a Hitachi S-2700 (Hitachi, Tokyo, Japan) electron microscope at 20 kV of accelerating voltage, using different magnifications.

Characterization of PEG-PLA Micelle Size and Zeta Potential

Following the self-assembly of the drug loaded micelles their size and zeta potential was determined by dynamic light scattering (DLS). Micelles samples analysis was performed at 25°C, by using a disposable folded capillary cell. All sample measurements were performed in a Zetasizer Nano ZS instrument (Malvern Instruments, Worcestershire, UK).

Evaluation of Drug Release Profile

Drug release was assessed using multiple samples of PEG-PLA micelles resuspended in PBS 1%, at pH 7.4 and 6.5, with a concentration of 0.1 mg/mL. Various samples were incubated at 37°C, under stirring, to collect data at different time points. After completing the time of incubation, each sample was centrifuged at 30,000 × *g* for 30 min for posterior UPLC analysis.

Cell Susceptibility to Blank Micelles

To evaluate micelle cytotoxicity, MCF-7 cells were initially seeded at a density of 8×10^3 cells/well in a 96-well flat bottom culture plates, containing DMEM-F12 supplemented with 10% FBS, as previously used by our group (33). Different concentrations of PEG-PLA blank micelles were tested, ranging between 5 and 2,000 μg/mL. Cell cytotoxicity was monitored by using the Resazurin assay as previously described (34). Fluorescence measurements were then performed in a plate reader spectrofluorometer (Spectramax Gemini XS, Molecular Devices LLC, USA).

Micelles Cellular Uptake Analysis

Characterization of micelle uptake was performed by flow cytometry. For uptake experiments, 6 well culture plates were seeded with 2×10^5 cells. To evaluate micelle cellular uptake, PEG-PLA micelles were prepared by self-assembly in order to encapsulate RITC (10 μM) that was used as model hydrophobic fluorescent probe. Labeled micelles were administered to MCF-7 cells for 2 and 4 h and removed afterwards by extensive rinsing with PBS. The cells were then recovered by trypsinization, pelleted and resuspended in 500 μL of PBS for flow cytometry analysis. All the experiments were performed on a BD FACSCalibur flow cytometer. Flow cytometry data was analyzed in FlowJo software (Treestar, Inc., CA, USA) and is presented as mean fluorescence intensity (MFI).

Micelle Intracellular Distribution in Breast Cancer Cells

Prior to confocal laser scanning microscopy (CLSM) experiments, RITC was encapsulated in the micellar carriers. 20×10^3 MCF-7 cells were seeded in μ-Slide 8 well imaging plates (Ibidi GmbH, Germany) and on the following day, cells were incubated with PEG-PLA/RITC micelles. After incubation, cells were fixed with 4% paraformaldehyde (PFA) for 15 min. MCF-7 cells were then permeabilized and incubated with a blocking solution. Afterwards, cells were incubated with the anti-F-actin Phalloidin CruzFluor® 647 conjugate antibody for 1 h, at room temperature (RT), followed by nuclear labelling with Hoechst 33342® (2 μM) nuclear probe. Imaging was performed in a Zeiss LSM 710 confocal microscope (Carl Zeiss SMT Inc., USA).

Anti-tumoral Activity of Drug-Loaded Micelles

MCF-7 cells were seeded as mentioned above and incubated with PL C and PL CS micelles, at a final drug concentration of 55.25 μM of Crizotinib and 40.33 μM of Sildenafil. Cell viability was determined at various time periods by incubating MCF-7 cells with the MTS, as previously described by our group (33).

Apoptosis Assay

MCF-7 cells were seeded as before mentioned in μ-Slide 8 well imaging plates (Ibidi GmbH, Germany). After 24 h in culture, the cells were incubated with PL CS micelles during 12 h. After micelle incubation, the cells were incubated with 7.5 μM of CellEvent™ Caspase-3/7 detection reagent during 30 min and visualized in a Zeiss LSM 710 microscope.

Statistical Analysis

One-way analysis of variance (ANOVA) with the post-hoc Newman-Keuls test was used to compare the results obtained for the different groups. A p value below 0.05 ($p < 0.05$) was considered statistically significant. The analysis of all data was performed in the GraphPad Prism v.5.0 software (Trial version, GraphPad Software, CA, USA).

RESULTS AND DISCUSSION

NMR Analysis of PEG-PLA Block Co-polymers

The ROP-based synthesis of PEG-PLA block co-polymers with different PLA chain lengths was analyzed through NMR spectroscopy. The ^{1}H NMR spectra obtained for the PEG-PLA block co-polymers is shown in Fig. 1. In this figure, the proton peaks appearing at $\delta = 5.2$ ppm and $\delta = 1.5$ ppm were assigned to the methyne (R_1-CH=R_2) and methyl (-CH_3) protons of the PLA monomers, respectively (28). The mPEG monomers possess a characteristic peak at approximately $\delta \approx 3.7$ ppm, that is assigned to methylene (=CH_2) protons (28). Moreover, the peak present at $\delta = 3.4$ ppm is correlated with the methyl (-CH_3) protons at the end of the mPEG polymer chain (28). The $CDCl_3$ characteristic peak ($\delta = 7.3$ ppm) was also obtained in all spectra.

The determination of the degree of polymerization and the Mn of the synthesized PLA polymer chain was also performed by ^{1}H NMR spectroscopy.

In addition, the synthesized co-polymers were also characterized by Fourier Transform Infrared Spectroscopy, X-ray

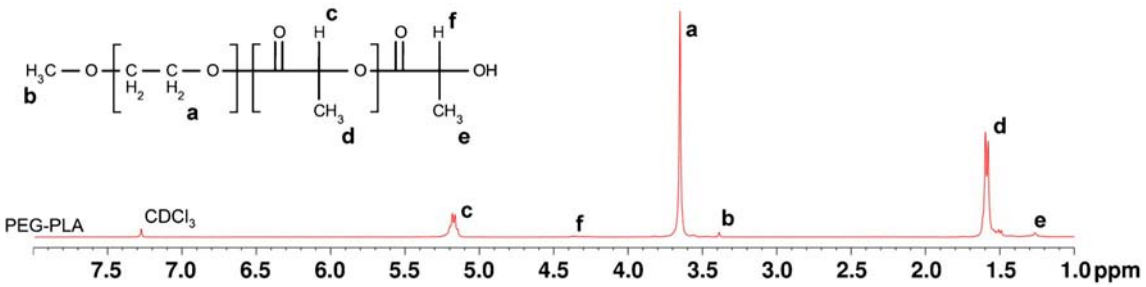

Fig. 1 ^{1}H NMR of the synthesized PEG-PLA block co-polymer.

Powder Diffraction, Differential Scanning Calorimetry and Gel Permeation Chromatography (See Supplementary Material, Methods section and Figures S1 to S4). As shown in Table I, the 8 h polymerization led to the formation of a PLA chain with Mn = 932 Da and a degree of polymerization of 160.46. The results obtained from the ROP polymerization indicate that the hydrophobic domain has a lower Mn than that of the hydrophilic segment of the co-polymer (Table I).

Generally, larger hydrophobic segments yield more stable micelles (35) however these carriers present higher crystallinity in the core, a factor that may affect biocompatibility and biodegradability (36). Therefore, in order to achieve a compromise between micelle stability and biological performance, this particular combination was chosen for the subsequent studies.

CMC Determination

The ability of PEG-PLA block co-polymers to form stable micelles with core-shell structures was evaluated by calculating their CMC. It is important to highlight that as potential drug delivery systems (DDS), PEG-PLA micelles must be stable at a low concentration, since otherwise after administration and contact with complex physiological media the carriers may disassemble (11). The obtained CMC results presented in Fig. 2, demonstrate that PEG-PLA micelles exhibit a very low CMC despite their relatively short hydrophobic segment. The values obtained for synthesized PEG-PLA micelles are similar to those generally reported in the literature (37).

These important findings indicate that the PEG-PLA co-polymers synthesized have the ability to form very stable micellar carriers at low polymer concentrations, thus having suitable characteristics for loading Crizotinib and Sildenafil (38).

Table I Degree of Polymerization, Mn of PLA and mPEG-PLA. Data is Presented as Mean ± s.d., $n = 5$

Polymerization time (h)	Degree of polymerization	PLA (Mn)	PEG-PLA Mn (PEG Mn = 2,000)
8	160.46	932 ± 4.06	2,932 ± 4.06

Hemocompatibility Assay

The blood hemocompatibility of the carriers was evaluated by incubating RBC's with the block co-polymer micelles to ascertain if there is any interference in the envisioned intravenous injection of PEG-PLA micelles. As shown in Fig. 3, the micellar carriers present supernatants similar to those of negative control (PBS). In contrast, the supernatant of the positive control is clearly red colored, indicating the release of hemoglobin by lysed RBC's. Moreover, as SEM micrographs demonstrate, the integrity of the RBC's morphology is maintained when incubated with the amphiphilic polymers (Fig. 3b).

The quantitative analysis indicates that PEG-PLA micelles do not promote RBC lysis, up to polymer concentrations of 500 μg/mL (Fig. 4). These results indicate that the different synthesized micelles are DDS with suitable properties for being used in therapeutic applications.

All values obtained for the percentage of hemolysis of RBC's in the presence of micelles have no significant difference to the negative control (PBS) as can be seen in Fig. 4. These results are within the percentage of hemolysis recommended by ISO/TR 7406 and ASTM F756 (39).

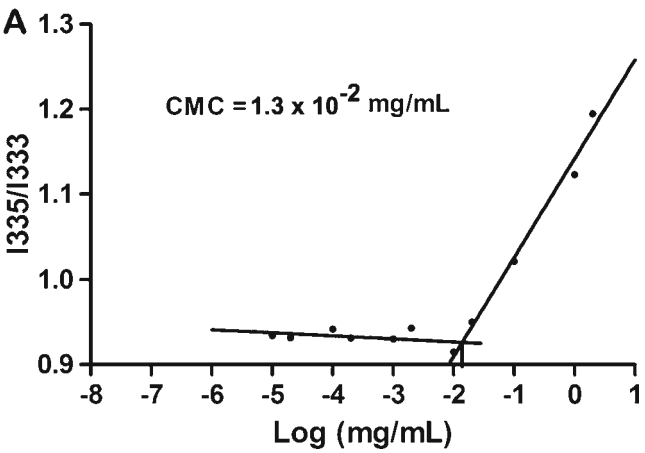

Fig. 2 CMC determination for: (**a**) PEG-PLA co-polymer micelles.

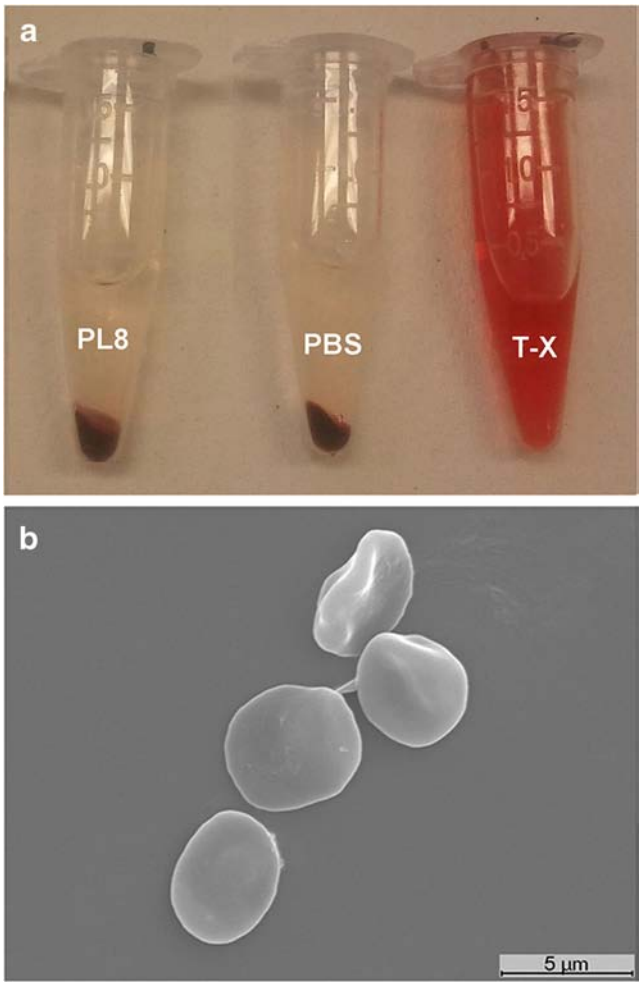

Fig. 3 Supernatants resulting from the hemolysis assay (**a**). Representative SEM image of RBC's previously incubated with PEG-PLA micelles (**b**). PBS and Triton-X100 (T-X) were used as negative and positive controls, respectively.

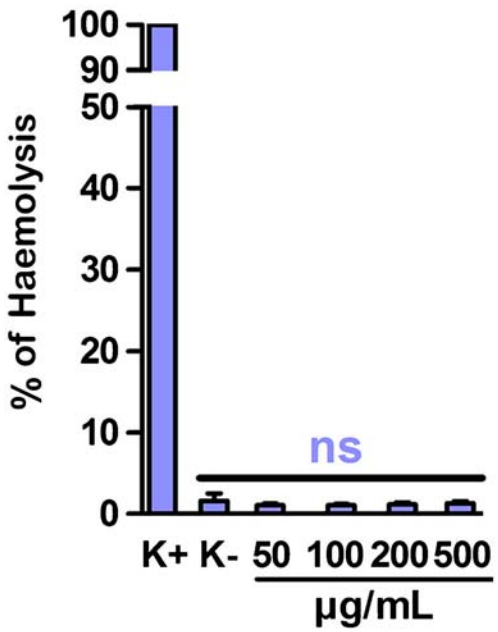

Fig. 4 Quantification of free heme groups (indicator of hemolysis) after incubation with synthesized PEG-PLA micelles. K+ (positive control) represents Triton X-100 treated RBC's, K− represents RBC's incubated with PBS. $n = 3$; *ns* non-significant.

Quantification of Single and Multiple Drug Encapsulation

The encapsulation of Crizotinib alone, or conjugated with Sildenafil inside micelles was evaluated by UPLC. All drug-loaded micelles were formulated with the film hydration-sonication method due to its enhanced loading capacity in comparison with other methods such as solvent evaporation or dialysis (29,40). For simplification PEG-PLA micelles were named as PL C and PL CS according to single or dual drug loading (Crizotinib and Crizotinib + Sildenafil). As the results in Fig. 5 show, the encapsulation efficiency of Crizotinib is above 95% for both PL C and PL CS, a value that is similar to that previously reported in the literature (41).

However it should be emphasized that the encapsulation efficiency of Crizotinib is remarkably high as shown in Fig. 5a. Moreover, Sildenafil is also loaded with an efficiency of 73%. These important findings support the concept that PEG-PLA drug loaded micelles are versatile systems for co-delivery of pharmaceutics. Encapsulating both Sildenafil and Crizotinib in micellar carriers improves their stability due to the establishment of drug-core hydrophobic interactions (35), and also increases their bioavailability inside cancer cells. Assuring this increased concentration in the cytoplasm is of critical importance since both drugs have intracellular target pathways. Promoting delivery into the local of action will thus influence the overall therapeutic outcome of the co-delivery approach.

Moreover, the ratio of Crizotinib/Sildenafil inside the micellar carriers is also fundamental for obtaining a synergistic effect, since if a low amount of Crizotinib is encapsulated no anti-tumoral effect would be obtained. On the other hand, even if Crizotinib encapsulation is sufficient, the amount of Sildenafil in the micellar formulation must be enough to inhibit the activity of ABC transporters, and avoid drug synergistic effect to become compromised (42). Achieving this balance during simultaneous drug encapsulation in the micellar carrier is challenging, but, as demonstrated by UPLC data, micelle self-assembly by the film hydration method, described in this study, promotes dual drug encapsulation with high efficiency and in a therapeutically relevant concentration, as demonstrated by *in vitro* data (Fig. 10). It is also important to emphasize that Crizotinib encapsulation efficiency is similar in PL and PL CS micelles, suggesting that the encapsulation of Sildenafil does not influence the amount of loaded Crizotinib under these conditions (Fig. 10).

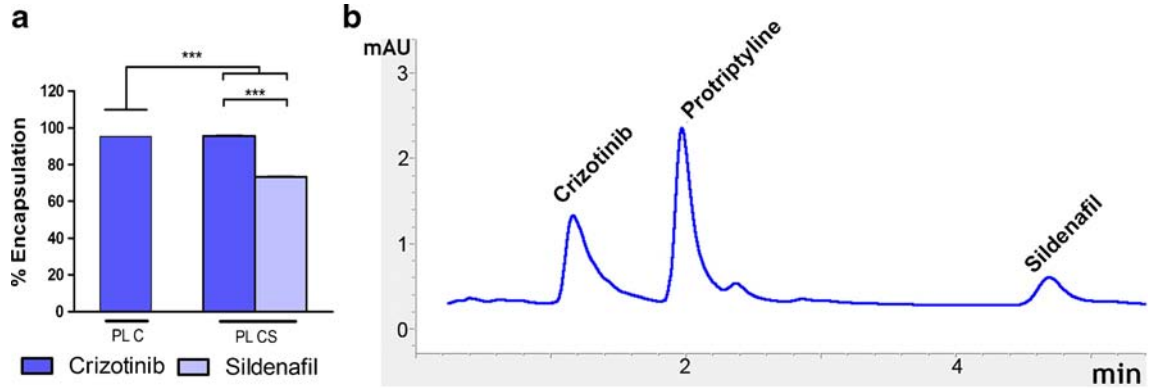

Fig. 5 (**a**) Determination of the encapsulation efficiency of Crizotinib and Crizotinib/Sildenafil combination in PEG-PLA micelles. $n = 3$; ***$p < 0.001$; *ns* non-significant; mean ± s.d. (**b**) Representative chromatogram of UPLC quantification. Protriptyline was used as an internal standard.

Morphological and Physicochemical Characterization of PEG-PLA Micelles

The DLS characterization results shows that the size PEG-PLA formulations ranges from 126 to 132 nm (Fig. 6). The drug-loaded micelles formulated with single or dual drugs present slightly lower size than those reported in the literature for these delivery systems (43). Moreover, the simultaneous inclusion of two drugs in the same micelles, did not increased its size substantially, as can be observed in Fig. 6. It is described that nanoparticles with less than 200 nm have a longer blood circulation time and nanoparticles larger than 250 nm are described to be extensively accumulated in organs such as the spleen, liver and lungs (44). Polydispersity index (PDI), of the produced micelles is under 0.25, indicating that these formulations present suitable size homogeneity for biomedical application, since a low dispersion is required for reproducible biological responses (45). Regarding the surface charge of the micelles, PEG-PLA micelles present a negative zeta potential. This finding is observed in both single and dual drug-loaded micelles (Fig. 6). These results are in accordance with those reported in the literature for PEG-PLA micelles, that commonly present zeta potential values in the range of +10 to −10 mV (43,46). The negative zeta potential values obtained for PEG-PLA provide an important advantage in respect to non-specific interactions with RBC's which impairs their function (47,48).

Micrographs analysis revealed the spherical-like morphology of all formulations analyzed. These results are corroborated by different studies in the literature that describe the formulation of PEG-PLA micelles as having spherical shape (49,50). Nanoparticle morphology is

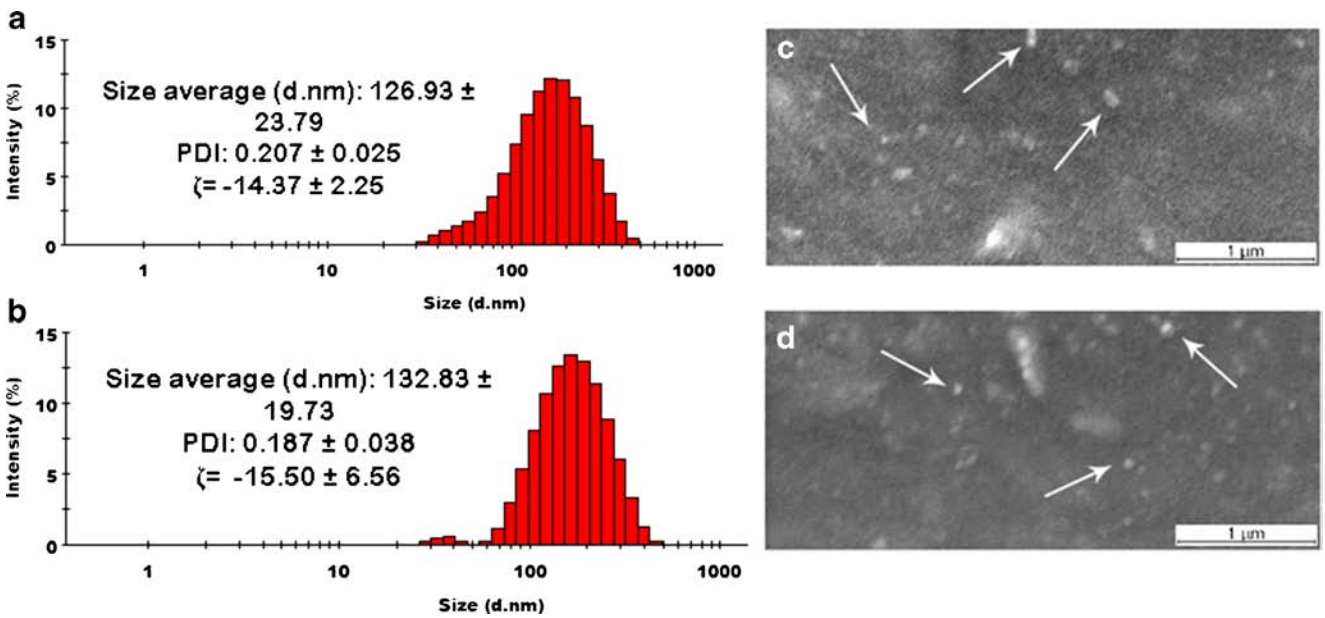

Fig. 6 Size, PDI and zeta potential of PL micelles loaded with drugs. PEG-PLA loaded with: Crizotinib (**a**) and with Crizotinib + Sildenafil (**b**). SEM micrographs of PEG-PLA micelles with encapsulated Crizotinib (**c**) and Crizotinib + Sildenafil (**d**). *White arrows* indicate micellar carriers. $n = 3$. Data is presented as mean ± s.d.

crucial to maximize cellular uptake. In this context, it has been described by Albanese *et al.* 2012, that spherical shape maximizes cellular uptake (48). Besides that, spherical form contributes for a better hydrodynamic behavior in the blood stream, an important fact if intravenous administration is envisioned (48).

Evaluation of Drug Release Profile

PEG-PLA micelles were able to sustain 80% of Crizotinib, resulting in a release of approximately 20% after 24 h (Fig. 7). The release line was kept for 8 days (data not shown), a result that is similar to that previously described in literature (51). On the other hand, Sildenafil appears to have a slightly faster release profile (Fig. 7). A first release of Sildenafil can be crucial to promote an immediate inhibition of ABC transporters, and in turn increase the anti-tumoral effect of slower released Crizotinib. The initial release of Sildenafil could however have some impact after intravenous administration (I.V.) of the micellar carriers since a slightly lower bioavailability could be obtained after administration via this particular route. However, several reports evidence that Sildenafil promotes an adjuvant anti-tumoral effect even when delivered in free drug formulation by I.V. (52). Moreover, other administration routes could be used for micelle delivery to breast cancer such as intratumoral in order to achieve maximum synergistic effect.

It is also important to emphasize that at an acidic pH, similar to that found in the tumor microenvironment, the release profile of both drugs is comparable to that obtained at pH 7.4.

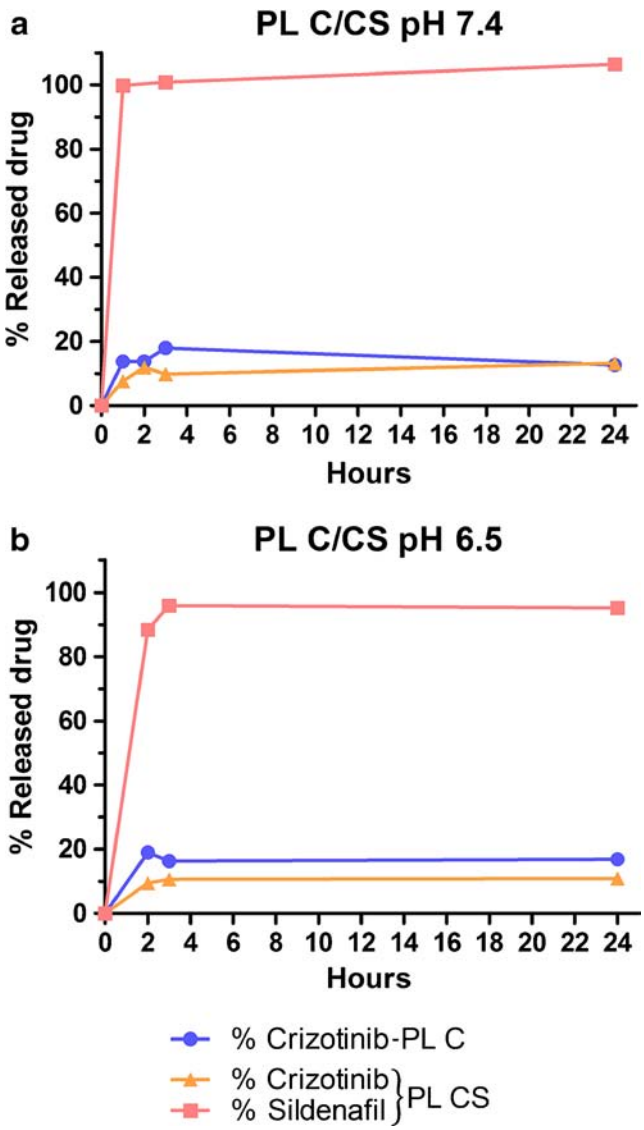

Fig. 7 Release profile of PEG-PLA formulations at physiologic pH (pH = 7.4) (**a**) and at the characteristic acidic tumor pH (pH = 6.5) (**b**). PL C/CS represents Crizotinib and Crizotinib + Sildenafil loaded PEG-PLA micelles.

Characterization of Micelle Cellular Uptake

Flow Cytometry Analysis

Characterization of micelle cellular uptake in MCF-7 breast cancer was evaluated after 2 and 4 h of micelle administration. No relevant difference in the percentage of cells containing micelles was obtained, for the two incubation times, 99.82% (2 h) and 98.02% (4 h). These results (Fig. 8c) suggest that after 2 h of incubation, almost all the MCF-7 cells had internalized some of the administered PEG-PLA micelles, indicating the suitability of these delivery systems to be applied in cancer therapy. On the other hand, flow cytometry data reveals that the MFI was increased from 92.2, at 2 h of incubation to 128.9, at 4 h of incubation, indicating that a longer incubation time, led to an increased accumulation of DDS inside breast cancer cells. The extensive uptake of drug loaded micelles is crucial to increase the synergistic effect of both drugs, since their main therapeutic targets are on the cell cytoplasm, namely, Sildenafil inhibits ABC transporters and Crizotinib inhibits c-MET/ALK phosphorylation (23,26).

To visualize cell internalization and intracellular distribution of PEG-PLA micelles, RITC-labelled micelles were administered to MCF-7 cells and then analysed by CLSM. In Fig. 8a and b the white arrows show the RITC-micelles internalized in MCF-7 cells, indicating that these are extensively localized in the cell cytoplasm. This is a very relevant finding since as before mentioned when the micelles start to release the drugs they will be available in their site of action, further improving the therapeutic effect.

Cytotoxicity Effect

PEG-PLA is described as a highly biocompatible block copolymer (53). Nevertheless, to further evaluate the biological properties of the synthesized materials, their cytotoxic profile

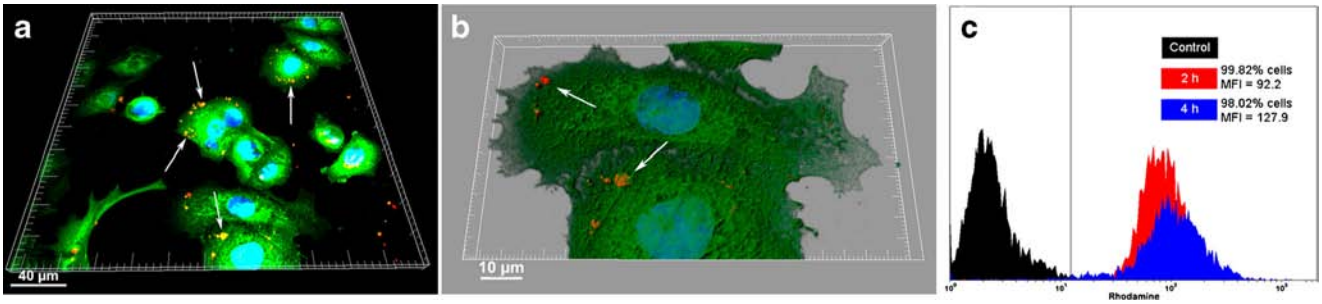

Fig. 8 CLSM images of MCF-7 cell with internalized PEG-PLA micelles encapsulating RITC. *White arrows* indicate micellar carriers. (**a**) 3D reconstruction of micelle cellular uptake; (**b**) High resolution 3D surface rendering of micelle uptake. *White arrows* indicate some of the labeled micelles internalized in MCF-7 Cells. (**c**) Overlaid cytometry histograms of MCF-7 cells incubated during 2 and 4 h with RITC-micelles. *Black* colour represents auto fluorescence of MCF-7 cells, *red* represents fluorescence of MCF-7 incubated during 2 h with RITC-micelles and *blue* shows incubation with the same RITC-micelles during 4 h. *Green* channel: F actin-Phalloidin alexa 647 antibody; *Blue* channel: Hoechst 33342®; *Red* channel: RITC-loaded micelles. *Yellow* color is the result of co-localization of RITC (*red*) and phalloidin-F-actin (*green*).

was characterized by using breast carcinoma cells (MCF-7) and normal human fibroblasts (Fib-H) (54).

The results presented in Fig. 9 show that the two tested cell lines present viability values above 95%, which are similar to that of K−. Both cell types maintained their viability in the presence of blank micelles up to concentrations of 2,000 µg/mL. The viability results obtained for Fib-H are particularly relevant since these indicate that the micellar carriers will not elicit deleterious effects in normal cells, thus reducing the overall cytotoxicity of this DDS after administration.

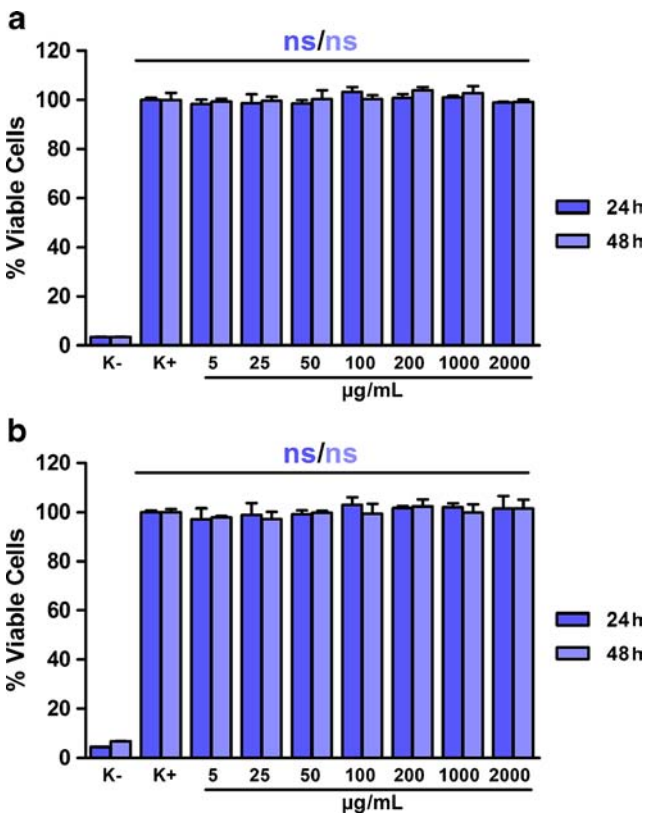

Fig. 9 Characterization of PEG-PLA micelles cytotoxicity for MCF-7 cells (**a**) and Fib-H (**b**). $n = 5$; *ns* non-significant. Data is presented as mean ± s.d.

Evaluation of the Synergistic Anti-tumoral Effect

The simultaneous administration of free Crizotinib and free Sildenafil was investigated, since it was initially postulated that

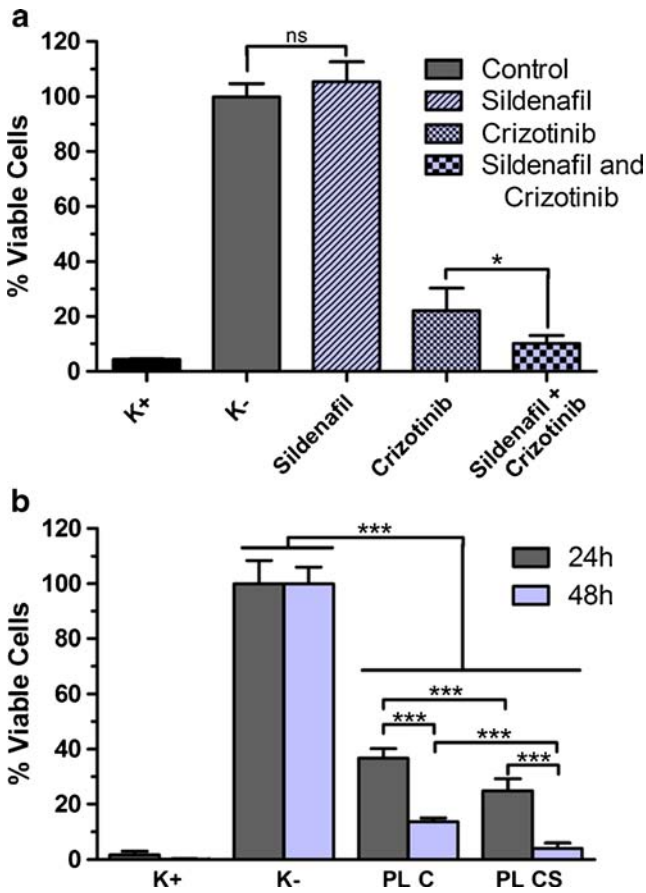

Fig. 10 (**a**) Evaluation of anti-tumoral activity of Crizotinib (alone) and Sildenafil (alone) and when Sildenafil was combined with Crizotinib after 48 h incubation. (**b**) Evaluation of the anti-tumoral activity of Crizotinib, Sildenafil and synergic effect between both, when delivery through PEG-PLA micelles. K+ is the positive control for cytotoxicity (dead cells). K− is the negative control (untreated cells). $n = 5$; ***$p < 0.001$; *ns* non-significant. Data is presented as mean ± s.d.

this novel combinatorial approach could further improve any anti-tumoral effect of Crizotinib in breast cancer cells. Initially the half maximal inhibitory concentration (IC50) was determined in order to evaluate the dose-response relationship after drug administration (Supplementary Material Figure S5).

As demonstrated by Fig. 10a, after 48 h, Sildenafil administration does not elicit any anti-tumoral effect. Actually, the MCF-7 cells incubated with Sildenafil alone, present a higher proliferation than non-incubated cells. On the other hand, the anti-tumoral effect of Crizotinib was markedly pronounced with only 22% of MCF-7 remaining viable after its administration. The simultaneous incubation of cells with Crizotinib and Sildenafil resulted in an abrupt decrease in cellular viability (only 10% of cells remained viable), when compared with the incubation of Crizotinib alone. Based on these results it is possible to conclude that their simultaneous administration will significantly improve the anti-tumoral outcome. This synergistic effect is likely correlated with the inhibitory effect of Sildenafil on several different drug transporters. This is a very important finding since in comparison with other ABC inhibition approaches, such as those dependent on siRNA, that only affect the expression of a single efflux transporter, Sildenafil has a wide inhibitory effect on several ABCs transporters simultaneously (42,55,56). This combinatorial approach may therefore open a new possibility to evaluate the inhibitory effect with other drug cocktails that target multiple intracellular pathways and ultimately reverse cell multi-drug resistance and promote their apoptosis. It is also important to emphasize that after free Sildenafil administration no cell death was observed in comparison with non-treated cells (Fig. 10a).

After establishing that there is an extensive synergistic effect associated with the use Crizotinib and Sildenafil, PEG-PLA micellar formulations containing both drugs were then incubated with MCF-7 breast cancer cells. When the drugs were delivered by micellar carriers to MCF-7 cells, a significant decrease in cell proliferation was observed for both single and dual drug formulations (Fig. 11b). Particularly, after only 24 h the PL C micelles decreased breast cancer cells viability up to 37% (Fig. 10b). More importantly, the administration of dual-loaded micelles reduced cell viability to 25%, after 24 h incubation, revealing that this combinational therapy administered through PEG-PLA micelles promotes an improved anti-tumoral effect. After 48 h, differences in cell viability in the single and dual micelle formulations were still observed (Fig. 10b). At this time, single-loaded PL C micelles promoted a decrease in MCF-7 cell viability levels up to 14%. Nonetheless, in the dual-loaded PL CS micelles cell viability levels decreased to about 4%, a significant difference that

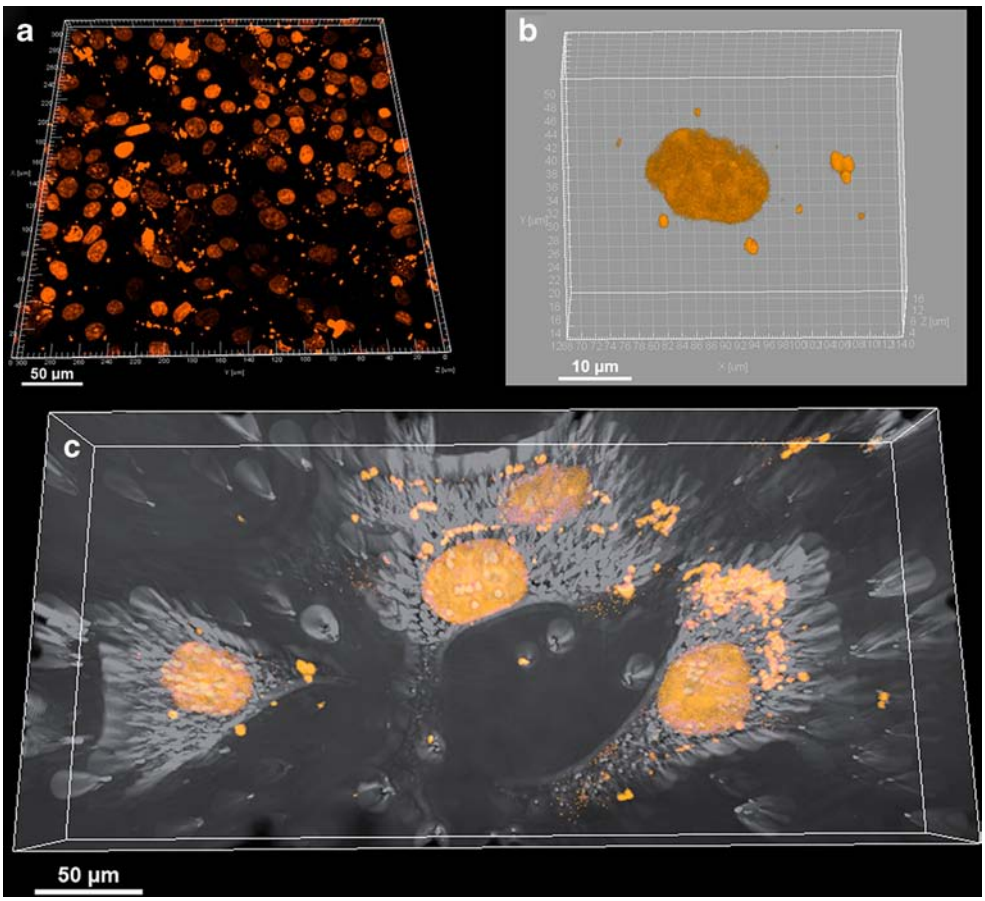

Fig. 11 CLSM images of apoptotic MCF-7 cells that were incubated 24 h with PL CS micelles. (**a**) 3D reconstruction of MCF-7 cell nucleus; (**b**) High resolution reconstruction of apoptotic cell nucleus; (**c**) Merged 3D image of MCF-7 cells. *Yellow* channel represents caspase-3 activated MCF-7 cells, derived from CellEvent ™ Caspase-3/7 detection probe.

undeniably illustrates the therapeutic potential of this co-delivery approach. These experiments were performed using only half of the dose of Crizotinib that was previously used in the free drug administration assays. This is a crucial finding if it is taken into account that in phase I clinical trials a range of 50 to 300 mg of Crizotinib must be administered to achieve a therapeutic effect in lung cancer cells (57). Our results show that encapsulating Crizotinib in PEG-PLA micelles significantly improves its intracellular bioavailability and that a smaller concentration of micelle-administered drug exhibits and improved therapeutic effect. This fact can thus impact the clinical trials underway for Crizotinib activity in cancer cells, but also evidence that this particular drug can be used in breast cancer therapy as well. Moreover, since it has been shown that Sildenafil further enhances the therapeutic effect by inhibiting ABC transporters an increased overall effect can be obtained. These results are in agreement with the therapeutic effect that Chen and co-workers reported in 2012 (55), when they manipulated the activity of P-gp (ABC1) and ABCC10/MRP7 proteins of MCF-7 cells, as an approach that led to an enhanced anti-tumoral effect of chemotherapy drugs (55). However, this approach is rather limited since only two ABC transporters were targeted. Furthermore, as can be observed in Fig. 10b, when both drugs are delivered through PEG-PLA micellar carriers the therapeutic outcome is enhanced, since a 2.7 fold reduction in MCF-7 cell viability was obtained, when Crizotinib and Sildenafil were simultaneous delivered by these DDS and with only half of the dose administered in free drug formulations.

Breast Cancer Cell Apoptosis

As an attempt to shed light on the biological events triggered by the use of Crizotinib in combination with Sildenafil in MCF-7 cancer cells, a fluorescence-based apoptosis assay was performed. As shown in Fig. 11, the incubation of dual-loaded PL CS micelles for 24 h induced caspase-3 and caspase-7 activation, since a bright yellow fluorescence was visualized. This signal is provided by a substrate that once cleaved by active caspase-3/7 emits fluorescence. This evidences the role of Crizotinib in promoting cell death trough apoptosis, that was also reported by Zhou *et al.* 2007 (23), emphasizing that this is a valuable approach to promote breast cancer cell death.

CONCLUSIONS

The straight forward research described in this work elucidates the synergistic effect between Crizotinib and Sildenafil against breast cancer cells, being even more pronounced when delivered through micellar carriers. The delivery of this drug combination either in nanomicelles or as free drugs has never been tested to the best of our knowledge. The results obtained showed the biocompatibility and hemocompatibility, of the synthesized block-copolymer micelles, providing important insights for their potential use in biomedical applications. In fact, it should be underlined that this delivery system is approved by FDA and European Medicines Agency. Both drugs used in this study were encapsulated with high efficiency on the synthesized micelles The synergistic effect obtained with Sildenafil and Crizotinib was observed when free drugs where incubated with MCF-7 cells. Remarkably, the anti-tumoral effect of this novel combination was significantly higher when the drugs were delivered to the intracellular compartment. These results emphasize that despite possessing a lower hydrophobic segment the PEG-PLA micelles achieved a compromise between stability, loading, biocompatibility and biological performance, thus indicating their potential for therapeutic applications.

This DDS can be further adapted to treat various types of cancers such as lung, cervix and liver cancer. I*n vivo* studies can also be performed on suitable mice models of breast cancer, in order to further demonstrate the applicability of these carriers loaded with both drugs. Further improvements regarding the controlled or stimuli responsive release of both Sildenafil and Crizotinib only in target breast cancer cells should also be investigated in the future in order to further improve the overall therapeutic effect of this novel drug combination. Moreover, this co-delivery approach can be extended to other combinatorial experiments that use more than two drugs.

ACKNOWLEDGMENTS AND DISCLOSURES

The authors would like to thank to Eng. Ana Paula for the acquisition of SEM images. This work was supported by the Portuguese Foundation for Science and Technology (FCT), (PTDC/EME-TME/103375/2008, PTDC/EBB-BIO/114320/2009, PEst-C/SAU/UI0709/2011). Vítor M. Gaspar, acknowledges a PhD fellowship from FCT (SFRH/BD/80402/2011).

REFERENCES

1. Siegel R, Naishadham D, Jemal A. Cancer statistics, 2013. CA Cancer J Clin. 2013;63:11–30.
2. Jemal A, Bray F, Center MM, Ferlay J, Ward E, Forman D. Global cancer statistics. CA Cancer J Clin. 2011;61:69–90.
3. Forouzanfar MH, Foreman KJ, Delossantos AM, Lozano R, Lopez AD, Murray CJL, *et al.* Breast and cervical cancer in 187 countries between 1980 and 2010: a systematic analysis. Lancet. 2011;378:1461–84.
4. Bhumbra R, Carter S, Jeys L, Tillman R, Abudu A, Sumathi V, *et al.* How does a poor response to chemotherapy affect outcomes in patients with osteosarcoma? J Bone Joint Surg (Br). 2012;94:38.

5. Liu R, Gilmore DM, Zubris KA, Xu X, Catalano PJ, Padera RF, *et al.* Prevention of nodal metastases in breast cancer following the lymphatic migration of paclitaxel-loaded expansile nanoparticles. Biomaterials. 2013;34:1810–9.
6. Smith IC, Heys SD, Hutcheon AW, Miller ID, Payne S, Gilbert FJ, *et al.* Neoadjuvant chemotherapy in breast cancer: significantly enhanced response with docetaxel. J Clin Oncol. 2002;20:1456–66.
7. Chen J, Wang L, Yao Q, Ling R, Li K, Wang H. Drug concentrations in axillary lymph nodes after lymphatic chemotherapy on patients with breast cancer. Breast Cancer Res. 2004;6:474–7.
8. Saha RN, Vasanthakumar S, Bende G, Snehalatha M. Nanoparticulate drug delivery systems for cancer chemotherapy. Mol Membr Biol. 2010;27:215–31.
9. Lila ASA, Eldin NE, Ichihara M, Ishida T, Kiwada H. Multiple administration of PEG-coated liposomal oxaliplatin enhances its therapeutic efficacy: a possible mechanism and the potential for clinical application. Int J Pharm. 2012;438:176–83.
10. Xu ZP, Zeng QH, Lu GQ, Yu AB. Inorganic nanoparticles as carriers for efficient cellular delivery. Chem Eng Sci. 2006;61:1027–40.
11. Rösler A, Vandermeulen GW, Klok H-A. Advanced drug delivery devices via self-assembly of amphiphilic block copolymers. Adv Drug Deliv Rev. 2012;53:95–108.
12. Letchfordand K, Burt H. A review of the formation and classification of amphiphilic block copolymer nanoparticulate structures: micelles, nanospheres, nanocapsules and polymersomes. Eur J Pharm Biopharm. 2007;65:259–69.
13. Garay-Jimenez JC, Young A, Gergeres D, Greenhalgh K, Turos E. Methods for purifying and detoxifying sodium dodecyl sulfate–stabilized polyacrylate nanoparticles. Nanomedicine: NBM. 2008;4:98–105.
14. Parveen S, Misra R, Sahoo SK. Nanoparticles: a boon to drug delivery, therapeutics, diagnostics and imaging. Nanomedicine: NBM. 2012;8:147–66.
15. Xiao L, Xiong X, Sun X, Zhu Y, Yang H, Chen H, *et al.* Role of cellular uptake in the reversal of multidrug resistance by PEG-b-PLA polymeric micelles. Biomaterials. 2011;32:5148–57.
16. Vogel CL, Cobleigh MA, Tripathy D, Gutheil JC, Harris LN, Fehrenbacher L, *et al.* Efficacy and safety of Trastuzumab as a single agent in first-line treatment of HER2-overexpressing metastatic breast cancer. J Clin Oncol. 2002;20:719–26.
17. Yezhelyev M, Gao X, Xing Y, Alhajj A, Nie S, Oregan R. Emerging use of nanoparticles in diagnosis and treatment of breast cancer. Lancet Oncol. 2006;7:657–67.
18. Drucker L, Afensiev F, Radnay J, Shapira H, Lishner M. Co-administration of simvastatin and cytotoxic drugs is advantageous in myeloma cell lines. Anticancer Drugs. 2004;15:79–84.
19. Gusman J, Malonne H, Atassi G. A reappraisal of the potential chemopreventive and chemotherapeutic properties of resveratrol. Carcinogenesis. 2001;22:1111–7.
20. Zhang L, Radovic-Moreno AF, Alexis F, Gu FX, Basto PA, Bagalkot V, *et al.* Co-delivery of hydrophobic and hydrophilic drugs from nanoparticle–aptamer bioconjugates. ChemMedChem. 2007;2:1268–71.
21. Lee AL, Wang Y, Cheng HY, Pervaiz S, Yang YY. The co-delivery of paclitaxel and Herceptin using cationic micellar nanoparticles. Biomaterials. 2009;30:919–27.
22. Shaw AT, Yasothan U, Kirkpatrick P. Crizotinib. Nat Rev Drug Discov. 2011;10:897–8.
23. Zou HY, Li Q, Lee JH, Arango ME, McDonnell SR, Yamazaki S, *et al.* An orally available small-molecule inhibitor of c-Met, PF-2341066, exhibits cytoreductive antitumor efficacy through antiproliferative and antiangiogenic mechanisms. Cancer Res. 2007;67:4408–17.
24. Zhou WJ, Zhang X, Cheng C, Wang F, Wang XK, Liang YJ, *et al.* Crizotinib (PF-02341066) reverses multidrug resistance in cancer cells by inhibiting the function of P-glycoprotein. Br J Pharmacol. 2012;166:1669–83.
25. Casaluce F, Sgambato A, Maione P, Ciardiello F, Gridelli C. Emerging mitotic inhibitors for non-small cell carcinoma. Expert Opin Emerg Drugs. 2013;18:97–107.
26. Limtrakul P, Chearwae W, Shukla S, Phisalphong C, Ambudkar SV. Modulation of function of three ABC drug transporters, P-glycoprotein (ABCB1), mitoxantrone resistance protein (ABCG2) and multidrug resistance protein 1 (ABCC1) by tetrahydrocurcumin, a major metabolite of curcumin. Mol Cell Biochem. 2007;296:85–95.
27. Zhang X, Li Y, Chen X, Wang X, Xu X, Liang Q, *et al.* Synthesis and characterization of the paclitaxel/MPEG-PLA block copolymer conjugate. Biomaterials. 2005;26:2121–8.
28. Li F, Li S, El Ghzaoui A, Nouailhas H, Zhuo R. Synthesis and gelation properties of PEG–PLA–PEG triblock copolymers obtained by coupling monohydroxylated PEG–PLA with adipoyl chloride. Langmuir. 2007;23:2778–83.
29. Gaucher G, Dufresne M-H, Sant VP, Kang N, Maysinger D, Leroux J-C. Block copolymer micelles: preparation, characterization and application in drug delivery. J Control Release. 2005;109:169–88.
30. Layekand B, Singh J. Amino acid grafted chitosan for high performance gene delivery: comparison of amino acid hydrophobicity on vector and polyplex characteristics. Biomacromolecules. 2013;14:485–94.
31. Akgül B, Lin K-W, Yang H-MO, Chen Y-H, Lu T-H, Chen C-H, *et al.* Garlic accelerates red blood cell turnover and splenic erythropoietic gene expression in mice: evidence for erythropoietin-independent erythropoiesis. PLoS One. 2010;5:e15358.
32. Pistos C, Papoutsis I, Dona A, Stefanidou M, Athanaselis S, Maravelias C, *et al.* Off-line HPLC method combined to LC-MS for the determination of sildenafil and its active metabolite in post-mortem human blood according to confirmation criteria. Forensic Sci Int. 2008;178:192–8.
33. Gaspar VM, Correia IJ, Sousa Â, Silva F, Paquete CM, Queiroz JA, *et al.* Nanoparticle mediated delivery of pure P53 supercoiled plasmid DNA for gene therapy. J Control Release. 2011;156:212–22.
34. Zakikhani M, Dowling R, Fantus IG, Sonenberg N, Pollak M. Metformin is an AMP kinase–dependent growth inhibitor for breast cancer cells. Cancer Res. 2006;66:10269–73.
35. Owen SC, Chan DP, Shoichet MS. Polymeric micelle stability. Nano Today. 2012;7:53–65.
36. Madhavan Nampoothiri K, Nair NR, John RP. An overview of the recent developments in polylactide (PLA) research. Bioresour Technol. 2010;101:8493–501.
37. He G, Ma LL, Pan J, Venkatraman S. ABA and BAB type triblock copolymers of PEG and PLA: a comparative study of drug release properties and "stealth" particle characteristics. Int J Pharm. 2007;334:48–55.
38. Fordeand PM, Rudin CM. Crizotinib in the treatment of non-small-cell lung cancer. Expert Opin Pharmacother. 2012;13:1195–201.
39. Yallapu MM, Ebeling MC, Jaggi M, Chauhan SC. Plasma proteins interaction with curcumin nanoparticles: implications in cancer therapeutics. Curr Drug Metab. 2013;14:504–15.
40. Pungkham H, Swatdipakdi N, Theerasilp M, Karnkla S, Chittchang M, Ploypradith P, *et al.* PEG-b-PCL and PEG-b-PLA polymeric micelles as nanocarrieres for lamellarin N delivery. Engineering in Medicine and Biology Society, EMBC, 2011 Annual International Conference of the IEEE2011. 2011;3245–8
41. Zhan C, Gu B, Xie C, Li J, Liu Y, Lu W. Cyclic RGD conjugated poly(ethylene glycol)-co-poly(lactic acid) micelle enhances paclitaxel anti-glioblastoma effect. J Control Release. 2010;143:136–42.
42. Shi Z, Tiwari AK, Patel AS, Fu L-W, Chen Z-S. Roles of sildenafil in enhancing drug sensitivity in cancer. Cancer Res. 2011;71:3735–8.

43. Vila A, Gill H, McCallion O, Alonso MJ. Transport of PLA-PEG particles across the nasal mucosa: effect of particle size and PEG coating density. J Control Release. 2004;98:231–44.
44. Owens III DE, Peppas NA. Opsonization, biodistribution, and pharmacokinetics of polymeric nanoparticles. Int J Pharm. 2006;307:93–102.
45. Asadi H, Rostamizadeh K, Salari D, Hamidi M. Preparation of biodegradable nanoparticles of tri-block PLA-PEG-PLA copolymer and determination of factors controlling the particle size using artificial neural network. J Microencapsul. 2011;28:406–16.
46. Gref R, Quellec P, Sanchez A, Calvo P, Dellacherie E, Alonso MJ. Development and characterization of CyA-loaded poly(lactic acid)–poly(ethylene glycol)PEG micro- and nanoparticles. Comparison with conventional PLA particulate carriers. Eur J Pharm Biopharm. 2001;51:111–8.
47. Cho W-S, Duffin R, Thielbeer F, Bradley M, Megson IL, MacNee W, *et al.* Zeta potential and solubility to toxic ions as mechanisms of lung inflammation caused by metal/metal oxide nanoparticles. Toxicol Sci. 2012;126:469–77.
48. Albanese A, Tang PS, Chan WC. The effect of nanoparticle size, shape, and surface chemistry on biological systems. Annu Rev Biomed Eng. 2012;14:1–16.
49. Jie P, Venkatraman SS, Min F, Freddy BYC, Huat GL. Micelle-like nanoparticles of star-branched PEO–PLA copolymers as chemotherapeutic carrier. J Control Release. 2005;110:20–33.
50. Zhang H, Xia H, Wang J, Li Y. High intensity focused ultrasound-responsive release behavior of PLA-b-PEG copolymer micelles. J Control Release. 2009;139:31–9.
51. Ayano E, Karaki M, Ishihara T, Kanazawa H, Okano T. Poly (N-isopropylacrylamide)–PLA and PLA blend nanoparticles for temperature-controllable drug release and intracellular uptake. Colloids Surf B: Biointerfaces. 2012;99:67–73.
52. Das A, Durrant D, Mitchell C, Mayton E, Hoke NN, Salloum FN, *et al.* Sildenafil increases chemotherapeutic efficacy of doxorubicin in prostate cancer and ameliorates cardiac dysfunction. Proc Natl Acad Sci. 2010;107:18202–7.
53. Hu K, Li J, Shen Y, Lu W, Gao X, Zhang Q, *et al.* Lactoferrin-conjugated PEG-PLA nanoparticles with improved brain delivery: in vitro and in vivo evaluations. J Control Release. 2009;134:55–61.
54. Gao MQ, Kim BG, Kang S, Choi YP, Park H, Kang KS, *et al.* Stromal fibroblasts from the interface zone of human breast carcinomas induce an epithelial-mesenchymal transition-like state in breast cancer cells in vitro. J Cell Sci. 2010;123:3507–14.
55. Chen JJ, Sun YL, Tiwari AK, Xiao ZJ, Sodani K, Yang DH, *et al.* PDE5 inhibitors, sildenafil and vardenafil, reverse multidrug resistance by inhibiting the efflux function of multidrug resistance protein 7 (ATP-binding Cassette C10) transporter. Cancer Res. 2012;103:1531–7.
56. Stege A, Priebsch A, Nieth C, Lage H. Stable and complete overcoming of MDR1/P-glycoprotein-mediated multidrug resistance in human gastric carcinoma cells by RNA interference. Cancer Gene Ther. 2004;11:699–706.
57. Camidge D, Bang Y, Kwak E, Shaw A, Iafrate A, Maki R, *et al.* Progression-free survival (PFS) from a phase I study of crizotinib (PF-02341066) in patients with ALK-positive non-small cell lung cancer (NSCLC). J Clin Oncol. 2011;29:2501.